Phonon-scattering spectra of $(Eu_{2/3}Ce_{1/3})_2(Ba_{2/3}Eu_{1/3})_2Cu_3O_9$ and $(Er_{2/3}Ce_{1/3})_2(Ba_{2/3}La_{1/3})_2Cu_3O_9$

Masashi Yoshida, Setsuko Tajima, Yuri Mizuo, Takahiro Wada, Ataru Ichinose, Yuji Yaegashi, Naoki Koshizuka, Hisao Yamauchi, and Shoji Tanaka

Superconductivity Research Laboratory, International Superconductivity Technology Center, 1-10-13 Shinonome, Koto-ku, Tokyo 135, Japan

(Received 31 October 1990; revised manuscript received 13 February 1991)

Raman-scattering spectra of $(Eu_{2/3}Ce_{1/3})_2(Ba_{2/3}Eu_{1/3})_2Cu_3O_9$ and $(Er_{2/3}Ce_{1/3})_2(Ba_{2/3}La_{1/3})_2Cu_3O_9$, both of which have Cu-$O_5$ pyramid structure, as well as $YBa_2Cu_3O_7$, have been observed at room temperature with use of single crystals. A scattering peak with B_{1g} symmetry has been observed at around 180 cm^{-1} and peaks with A_{1g} symmetry at around 220, 290, 450, and 540 cm^{-1}, in both compounds. The 180-cm^{-1} peak with B_{1g} symmetry is assigned to the out-of-phase bending of oxygen in the Cu-O_2 plane and the 540-cm^{-1} peak with A_{1g} symmetry to the stretching of apical oxygen. Phonon-energy calculation has been performed with use of ionic potentials obtained for $YBa_2Cu_3O_7$. To explain the observed B_{1g} phonon energies, it has been found that the polarizability of the oxygen in the Cu-O_2 plane in these compounds must be increased in relation to that in $YBa_2Cu_3O_7$. The 220- and 290-cm^{-1} peaks are tentatively assigned to the mixed vibrational modes of oxygens in the Cu-O_2 plane and lanthanide atoms.

I. INTRODUCTION

Since the discovery of superconductivity in $La_{2-x}Ba_xCuO_4$ by Bednorz and Müller,[1] many other cuprate superconductors have been found. According to the oxygen coordination around Cu atom, they can be classified into three groups: the first group which includes compounds with Cu-O_6 octahedron structure ($La_{2-x}Sr_xCuO_4$, $Bi_2Sr_2CuO_x$, $Tl_2Ba_2CuO_x$ etc.); a second group of compounds with Cu-O_5 pyramid structure [$YBa_2Cu_3O_7$, $Bi_2Sr_2Ca_{n-1}Cu_nO_{4+2n}$ ($n=2,3$), $Tl_2Ba_2Ca_{n-1}Cu_nO_{4+2n}$ ($n=2,3$), etc.]; and a third group of compounds with Cu-O_4 plane structure ($Pr_{2-x}Ce_xCuO_4$, etc.).[2] The structures and the superconducting transition temperatures (T_c's) of cuprate superconductors are summarized in Ref. 2. T_c depends critically on the Cu-O complexes, and compounds with the Cu-O_5 pyramid have the highest T_c's.

Much attention has been focused on the elementary excitations associated with the Cu-O complexes because they are assumed to play a major role in the superconductivity. Various theoretical models[3] have been proposed for the attractive electron-electron interaction causing Cooper-pair formation, among which is the conventional BCS phonon-mediated mechanism.[4,5] It has been pointed out that superconductivity up to 90 K is attainable by a phonon mechanism due to strong electron-phonon coupling in the cuprate superconductors.[5]

Raman spectra of cuprate superconductors have been investigated intensively to clarify the role of phonons in the superconductivity. In $YBa_2Cu_3O_x$, several phonon modes associated with the Cu-O_5 pyramid have been identified,[6] and some of them have been found to change their energies around T_c.[7]

Recently, Sawa *et al.* found another superconductor family $(L_{2/3}Ce_{1/3})_2(Ba_{2/3}L_{1/3})_2Cu_3O_9$ (L=Nd, Sm, or Eu),[8] which has the Cu-O_5 pyramid structure as well as $YBa_2Cu_3O_7$. The superconducting transition temperature T_c is around 30 K,[8] which is much lower than that of $YBa_2Cu_3O_7$ (92 K).

Figure 1 shows primitive unit cells of $(Eu_{2/3}Ce_{1/3})_2(Ba_{2/3}Eu_{1/3})_2Cu_3O_9$ (hereafter we abbreviate as Eu 2:2:3) and $YBa_2Cu_3O_7$ (Y 1:2:3). Both of them contain two Cu-O_5 pyramids. They are very similar to each other except for the following points. (i) In Eu 2:2:3 there are two Eu (Ce) layers and an oxygen layer between them while only one Y layer in Y 1:2:3. (ii) In the Cu(1)-O plane of Eu 2:2:3, oxygen atoms populate randomly with occupancy of 0.5, while in the Cu(1)-O plane of Y 1:2:3, oxygen atoms align along the a axis. In addition, there is a difference in the stacking of the primitive cell along the c direction. In Eu 2:2:3 the primitive cells are

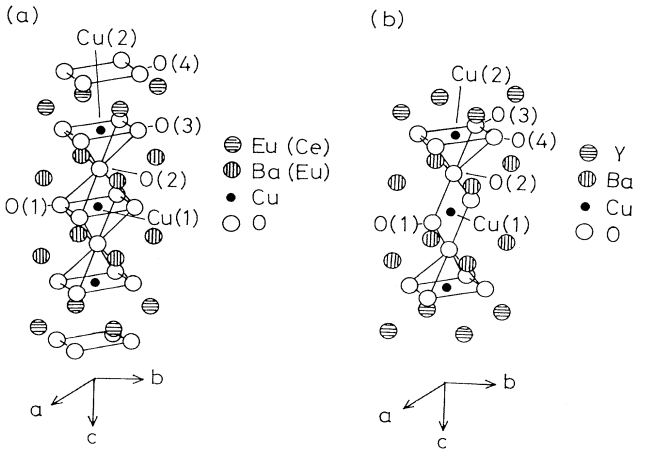

FIG. 1. Crystal structure of (a) $(Eu_{2/3}Ce_{1/3})_2(Ba_{2/3}Eu_{1/3})_2Cu_3O_9$ and (b) $YBa_2Cu_3O_7$.

stacked with the displacement (0.5,0.5) in the *a-b* plane, while there is no such displacement in Y 1:2:3.

In the 2:2:3-type compounds, there are two different sites of lanthanide ions. Wada *et al.* synthesized $(Gd_{2/3}Ce_{1/3})_2(Ba_{2/3}La_{1/3})_2Cu_3O_9$ and found that a Gd ion with a small radius occupies an A_1 site together with a Ce ion and a La ion with a large radius occupies an A_2 site together with a Ba ion.[9]

In the present study, we measured polarized Raman spectra of superconducting and semiconducting Eu 2:2:3 and semiconducting $(Er_{2/3}Ce_{1/3})_2(Ba_{2/3}La_{1/3})_2Cu_3O_9$ (Er-La 2:2:3) using single crystals at room temperature. We obtained scattering peaks due to phonons associated with the Cu-O_5 pyramid. A preliminary phonon-energy calculation was performed based on the shell model and the phonon-mode assignments were given. The difference of the phonons between these compounds and Y 1:2:3 was discussed.

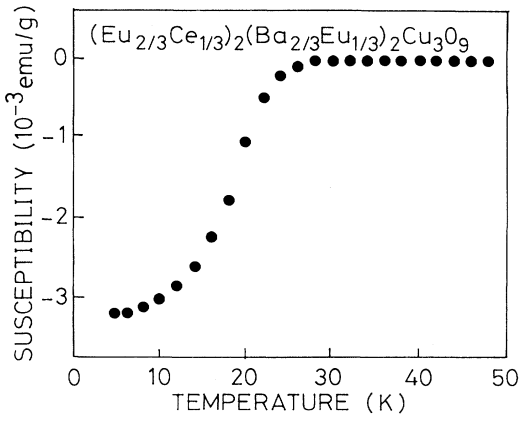

FIG. 2. Zero-field-cooled SQUID magnetometry data taken in a 10-Oe field of a typical single crystal of $(Eu_{2/3}Ce_{1/3})_2(Ba_{2/3}Eu_{1/3})_2Cu_3O_9$ used in this study.

II. EXPERIMENT

Single crystals of Eu 2:2:3 and Er-La 2:2:3 were grown with a small excess of copper oxide serving as the flux. Powders of Eu_2O_3, Er_2O_3, La_2O_3, CeO_2, $BaCO_3$, and CuO with purity of 99.99% were mixed with a cation ratio of

[Eu]:[Ce]:[Ba]:[Cu]=2:0.67:1.33:3.5

([Er]:[Ce]:[Ba]:[La]:[Cu]=1.33:0.67:1.33:0.67:3.5) .

They were placed in platinum crucibles and were heated to 1400 °C in air, held for 10 h, and then cooled down to 1100 °C. After that, they were cooled gradually to 800 °C at a rate of 2 °C/h and then furnace cooled to room temperature. The dimensions of the obtained single crystals were about $1\times1\times0.1$ mm^3. They were annealed at 500 °C in 400 atmospheric oxygen pressure for 5 h to obtain superconducting samples.

With a single-crystal x-ray diffractometer, we found the crystals to be oriented with the *c* axis perpendicular to the large surface of the platelet. The lattice parameters of Eu 2:2:3 were $a=b=3.855$ Å and $c=28.56$ Å, and those of Er-La 2:2:3 were $a=b=3.870$ Å and $c=28.55$ Å. Figure 2 shows the temperature dependence of the magnetic susceptibility of Eu 2:2:3 measured with a superconducting quantum interference device (SQUID) magnetometer. The measurement was performed by cooling the sample down to 4 K, applying a magnetic field of 10 Oe, and increasing the temperature. The superconducting transition temperature of our sample was about 30 K, which was nearly the same as that of sintered materials.[8] On the other hand, Er-La 2:2:3 samples do not show superconductivity even after high-pressure oxygen treatment. Semiconducting Eu 2:2:3 samples were obtained by annealing the superconducting samples at 600 °C in a N_2 environment for 2 days.

Raman spectra were observed at room temperature in the backscattering configuration using 5145-Å light from an Ar laser. The incident beam was focused on the sample surface with a diameter of about 0.1 mm. The laser power was maintained below 50 mW to avoid damaging the samples. The scattered light was detected with a double monochromator Jobin Yvon U-1000 and a photon-counting detection system with a photomultiplier Hamamatsu R-943. Spectral resolution was 3 cm^{-1}.

III. SYMMETRY ANALYSIS OF THE VIBRATIONAL MODES

The 2:2:3-type compounds have a body-centered tetragonal structure with space group $I4/mmm$.[8] We have carried out a symmetry analysis of the vibrational modes of the 2:2:3-type compounds based on the structure model shown in Fig. 1. The primitive cell contains 17 atoms [or 16 atoms considering the occupancy of 0.5 in the O(1) sites]. Optical phonons at the Γ point are composed of

$$\Gamma=5A_{1g}+B_{1g}+6E_g+3B_{2u}+7A_{2u}+10E_u ,$$

where A_{1g}, B_{1g}, and E_g modes are Raman active, and A_{2u} and E_u modes are ir active, while B_{2u} modes are inactive. The symmetries of the modes associated with the motion of particular atoms are given in Table I.

In Fig. 3 are shown schematically the displacements of atoms in the A_{1g} and B_{1g} modes. The A_{1g} and B_{1g} modes are composed of the displacements of Eu (Ce), Cu(2), Ba (Eu), O(2), and O(3) atoms along the *c* axis. Among the A_{1g} and B_{1g} modes, oxygen vibration modes

TABLE I. Configuration of modes associated with displacements of atoms at specific sites in $(Eu_{2/3}Ce_{1/3})_2(Ba_{2/3}Eu_{1/3})_2Cu_3O_{10}$.

Atoms	Mode classification
Cu(1)	$A_{2u}+E_u$
Cu(2)	$A_{1g}+E_g+A_{2u}+E_u$
Eu	$A_{1g}+E_g+A_{2u}+E_u$
Ba	$A_{1g}+E_g+A_{2u}+E_u$
O(1)	$B_{2u}+A_{2u}+2E_u$
O(2)	$A_{1g}+E_g+A_{2u}+E_u$
O(3)	$A_{1g}+B_{1g}+2E_g+A_{2u}+B_{2u}+2E_u$
O(4)	$A_{2u}+B_{2u}+2E_u$

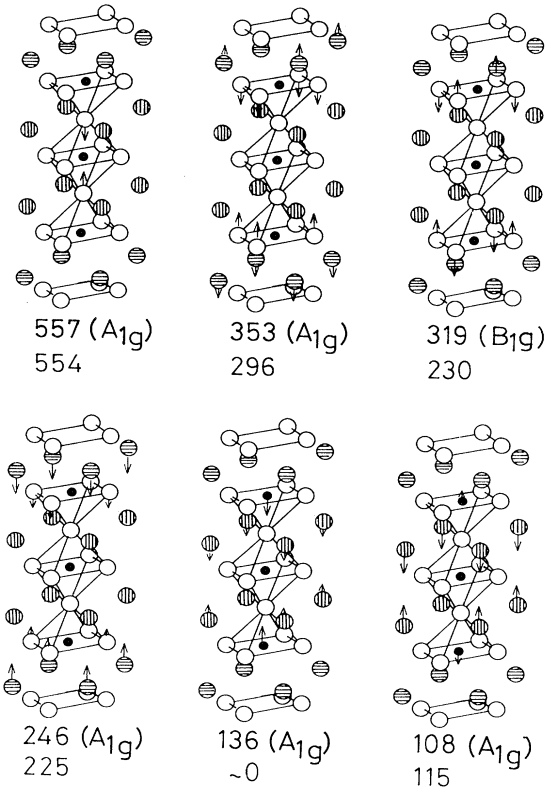

FIG. 3. Eigenvectors of A_{1g} and B_{1g} modes of $(Eu_{2/3}Ce_{1/3})_2(Ba_{2/3}Eu_{1/3})_2Cu_3O_9$. The calculated phonon energies are shown below each mode in units of cm^{-1} using a core-shell force constant of O(3), $k=310$ (upper) and $k=190$ (lower).

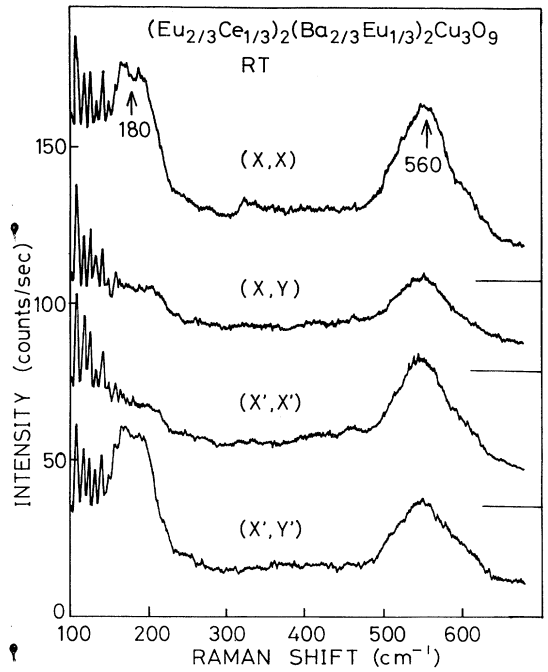

FIG. 4. Raman spectra taken on the *a-b* plane of a superconducting $(Eu_{2/3}Ce_{1/3})_2(Ba_{2/3}Eu_{1/3})_2Cu_3O_x$ crystal for (X,X), (X,Y), (X',X'), and (X',Y') geometries.

associated with the Cu-O_5 pyramid are the stretching vibration of O(2) along the c axis (A_{1g}) and the in-phase (A_{1g}) and out-of-phase (B_{1g}) bending vibrations of O(3) along the c axis. It should be noted that, in Eu 2:2:3, coupling of the vibration of Eu (Ce) and O(3) atoms occurs in the A_{1g} symmetry vibration, which brings about two eigenmodes associated with in-phase motion of O(3); in one of them, Eu (Ce) and O(3) atoms move in the same direction, and in the other, the opposite direction (see Fig. 3).

Scattering due to A_{1g}-mode phonons is allowed in the (Z,Z), (X,X), and (X',X') geometries where (I,I) $(I=Z,X,X')$ refers to the polarization of the incident and scattered lights along the I axis. X, Y, and Z refer to polarization along the crystallographic a, b, and c axes, respectively. The X' (Y') is the direction rotated 45° around the Z axis from the X (Y) axis. The B_{1g}-mode phonon is active in the (X',Y') geometry, and E_g-mode phonons are active in the (Z,X) geometry.

IV. RESULTS

Figure 4 shows the polarized Raman spectra taken on the *a-b* plane of a superconducting Eu 2:2:3 sample for the (X,X), (X,Y), (X',X'), and (X',Y') geometries. In Fig. 4 sharp peaks around 100 cm^{-1} are due to vibration of oxygen molecules in the air. A broad peak is seen at around 180 cm^{-1} in the spectrum for the (X,X) and (X',Y') geometries, while not for the (X,Y) and (X',X'), exhibiting B_{1g} symmetry. Since there exists only one B_{1g}-mode phonon, we can identify it as the out-of-phase vibration of the O(3) atoms along the c axis unambiguously. It should be noted the that B_{1g} phonon energy of Eu 2:2:3 is considerably smaller than that of Y 1:2:3 (330 cm^{-1}).[6] On the other hand, a peak is seen at 560 cm^{-1} in any spectrum in Fig. 4. This peak is supposed to appear due to defects. The origin of the 560 cm^{-1} peak will be discussed in Sec. V.

Figure 5 shows the polarized Raman spectra taken on

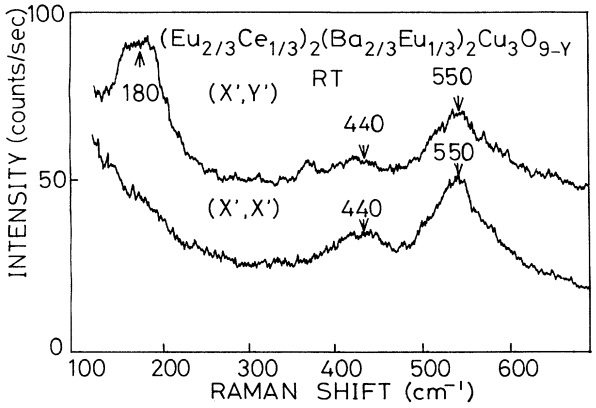

FIG. 5. Raman spectra taken on the *a-b* plane of a semiconducting $(Eu_{2/3}Ce_{1/3})_2(Ba_{2/3}Eu_{1/3})_2Cu_3O_{9-y}$ crystal for (X',X') and (X',Y') geometries.

the a-b plane of a semiconducting Eu 2:2:3 sample for (X',X') and (X',Y') geometries. Peaks are seen at 180, 440, and 550 cm^{-1} in the (X',Y') geometry and at 440 and 550 cm^{-1} in the (X',X') geometry. The 180-cm^{-1} peak rarely shifts in the semiconducting sample in comparison with the superconducting one. On the other hand, the 560-cm^{-1} peak shifts to the lower-energy side by 10 cm^{-1}. The 440-cm^{-1} peak is supposed to be due to defects as well as the 550-cm^{-1} peak.

Figures 6(a) and 6(b) show the polarized Raman spectra taken on the a-c plane of a superconducting and semiconducting Eu 2:2:3 sample, respectively, for the (Z,Z) and (X,Z) geometries. In Fig. 6(a) prominent peaks are seen in the (Z,Z) geometry at 445 and 543 cm^{-1} and weak structures at around 217 and 290 cm^{-1}. These peaks are not seen in the (X,Z) geometry, exhibiting A_{1g} symmetry. No peak is seen in the (X,Z) geometry where E_g-mode phonons are Raman allowed.

In the Raman spectra of Y 1:2:3, prominent peaks with A_g symmetry are seen at 500 and 440 cm^{-1}, where the former is assigned as the vibration of O(2) along the c axis and the latter the in-phase vibrations of O(3) and O(4) along the c axis.[6] The 543-cm^{-1} peak in Eu 2:2:3 can be assigned to the vibration of O(2) along the c axis. On the other hand, it is uncertain that the 445-cm^{-1} peak is due to in-phase vibration of O(3) along the c axis since it is unlikely that the energy of the out-of-phase vibration of O(3) of Eu 2:2:3 (180 cm^{-1}; see Fig. 4) is considerably lower than that of Y 1:2:3, while the in-phase vibration of O(3) is kept to nearly the same energy. We will disucss this point in detail in Sec. V.

In Fig. 6(b) prominent peaks are seen for the (Z,Z) geometry at 452 and 543 cm^{-1} and weak structures at 215 and 280 cm^{-1}. These peak energies are nearly the same as those observed in the superconducting sample. In the case of Y 1:2:3, the 500-cm^{-1} peak shifts to the lower-energy side by 25 cm^{-1} as the oxygen composition decreases from 7 to 6.[6] Such an energy shift of the stretching mode of O(2) has not been observed in Eu 2:2:3. On the other hand, in the spectrum of the semiconductng sample, a shoulder is seen on the higher-energy side of the 543-cm^{-1} peak. In the semiconducting sample, the occupancy of the oxygen in the Cu(1)-O plane decreases, which may enhance disorder scattering. The shoulder may be caused by the stretching vibrations of O(2) with $k \neq 0$, which become allowed as a result of disorder.

Figures 7(a) and 7(b) show the polarized Raman spectra taken on the a-b and a-c planes, respectively, of semiconducting Er-La 2:2:3. In Fig. 7(a) a peak is seen at 170 cm^{-1} for the (X',Y') geometry and not for the (X',X') geometry exhibiting B_{1g} symmetry. A defect-induced peak is seen at 560 cm^{-1} both in the (X',Y') and (X',X') geometries. These features are similar to those in superconducting and/or semiconducting Eu 2:2:3 (Figs. 4 and 5).

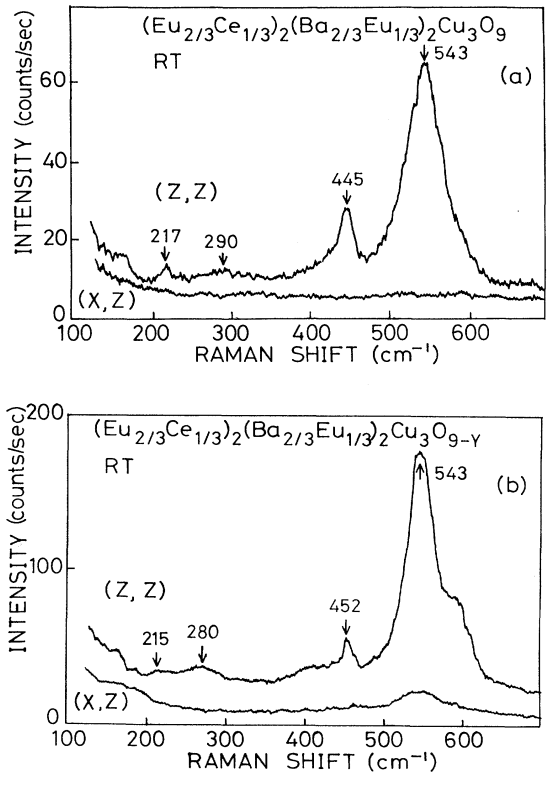

FIG. 6. Raman spectra taken on the a-c plane of (a) a superconducting and (b) a semiconducting $(Eu_{2/3}Ce_{1/3})_2(Ba_{2/3}Eu_{1/3})_2Cu_3O_x$ crystal for (Z,Z) and (Z,X) geometries.

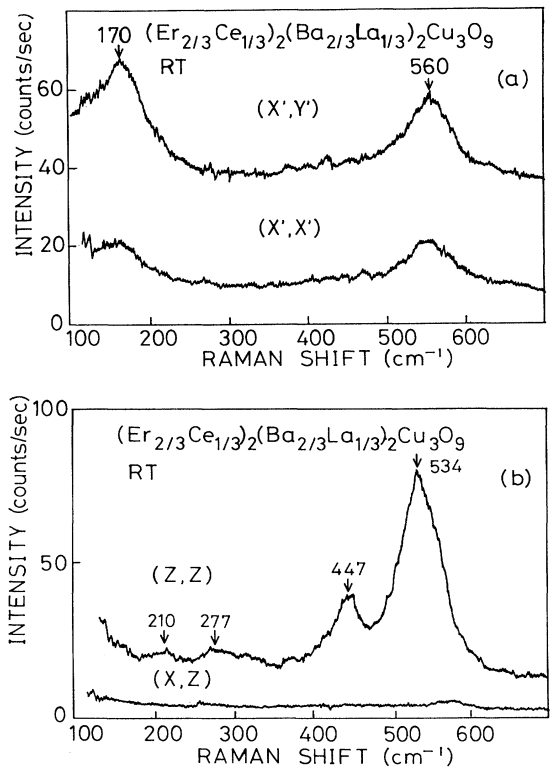

FIG. 7. Raman spectra taken on the (a) a-b plane and (b) a-c plane of a semiconducting $(Er_{2/3}Ce_{1/3})_2(Ba_{2/3}La_{1/3})_2Cu_3O_9$ crystal.

In Fig. 7(b) prominent peaks are seen at 447 and 534 cm^{-1} and weak structures at 210 and 277 cm^{-1} for the (Z,Z) geometry. These peaks are not seen for the (X,Z) geometry. These features are similar to those of superconducting and/or semiconducting Eu 2:2:3 (Figs. 5 and 6).

V. DISCUSSION

In the previous section, we showed scattering spectra of Eu 2:2:3 and Er-La 2:2:3. We have found that the B_{1g}-symmetry peak energies of these compounds are considerably lower than that of Y 1:2:3, while the A_{1g}-symmetry peak energies are nearly the same.

Phonon-mode assignments of Y 1:2:3 have been performed on the basis of phonon-energy calculations using force constants[10] or interaction potentials.[11] Between them, the method using interaction potentials has a priority that the potentials depend only on the ionic species and not on the spatial arrangements of ions in the crystal. We performed phonon-energy calculations of Eu 2:2:3 using the pair potential method with potentials obtained for Y 1:2:3 in order to identify the Raman peaks and also to clarify the origin of the difference of the B_{1g}-mode phonon energy between Y 1:2:3 and the 2:2:3-type compounds.

We assumed a short-range Born-Mayer-type potential and a long-range Coulomb potential. The Born-Mayer potentials are represented as

$$V_{ij}(r)=a_{ij}\exp(-b_{ij}r) ,$$

where i,j label the ions and r is their distance. The deformation of the electronic charge density induced by the displacement of the ions was treated in the framework of a shell model. Electronic displacement is represented using shell charge Y_i and on-site core-shell force constant k_i. We used the values of a_{ij}, b_{ij}, k_i, and Y_i obtained by Kress *et al.*[11] for Y 1:2:3. These values are summarized in Table II. We applied the values for Y and Ba sites in Y 1:2:3 to that for Eu and Ba sites in Eu 2:2:3, respectively. The ionic charge of oxygen atoms is fixed to -1.8 as in Ref. 11, while charges at Eu and Ba sites are changed (increased) from those at Y and Ba sites in Y 1:2:3 to conserve the charge neutrality.

As the crystal structure, we choose that of $(Sm_{2/3}Ce_{1/3})_2(Ba_{2/3}Sm_{1/3})_2Cu_3O_x$ determined by Wada *et al.*[9] In order to take into account the fact that the occupancy of the O(1) site is 0.5, we assumed an orthorhombic structure where oxygen atoms are aligned along the a direction. By this assumption, no significant change of phonon energies occurs except those associated with Cu(1) and O(1).

The calculated A_{1g}- and B_{1g}-mode phonon energies are shown in Fig. 3. The calculated value of 557 cm^{-1} for the stretching vibration of O(2) along the c axis agrees well with the observed value of 543 cm^{-1} (Fig. 6) (or 534 cm^{-1} of Er-La 2:2:3, Fig. 7). The observed energy of this mode is about 40 cm^{-1} higher than the corresponding one of Y 1:2:3. This is mainly caused by the fact that the Cu(1)-O(2) distance in Eu 2:2:3, 1.761 Å,[9] is considerably shorter than that in Y 1:2:3, 1.846 Å.[12] Sawa *et al.* measured x-ray-diffraction spectra of Eu 2:2:3 and determined the atomic positions.[8] According to them, the Cu(1)-O(2) distance is 1.878 Å, which is longer than that in Y 1:2:3. However, their results cannot explain the shift of the O(2) vibration of Eu 2:2:3 to the higher-energy side in comparison with that of Y 1:2:3.

The calculated energies of the in- and out-of-phase vibrations of O(3) are 353 and 319 cm^{-1}, respectively. These calculated values are considerably different from the experimental value 180 cm^{-1} (or 170 cm^{-1} of Er-La 2:2:3). The energies of these two phonon modes are determined mainly by the Born-Mayer interaction of O(3) with Eu and Ba, Coulomb interaction of O(3) with Cu(2), and the dynamical screening on the O(3) atoms. However, it is not likely that parameter values for Born-Mayer or Coulomb interaction differ drastically between Y 1:2:3 and Eu 2:2:3 taking into account the static stability of the structure. Thus the lower energy of the B_{1g}-mode phonon energy of Eu 2:2:3 compared with that of Y 1:2:3 cannot be explained merely by the change of the atomic configurations.

To explain the observed value 180 cm^{-1} of the out-of-

TABLE II. Parameters used in the phonon-energy calculation of $(Eu_{2/3}Ce_{1/3})_2(Ba_{2/3}Eu_{1/3})_2Cu_3O_x$. a and b, Born-Mayer constants; Z, Y, and k, ionic charge, shell charge, and on-site core-shell force constant of the ion (v_a: volume of the primitive cell). Anisotropic polarizability is assumed for O(1) and O(2) with force constants $k(\|)$ (parallel to the Cu-O direction) and $k(\perp)$ (perpendicular to the Cu-O direction).

	a (eV)	b (Å^{-1})		Z/e	Y/e	k (unit of e^2/v_a)
Eu-O	3010	2.90	Eu	3.10	−1.42	1074
Ba-O	3225	2.90	Ba	2.00	2.32	203
Cu(1)-O	1260	3.45	Cu(1)	2.00	3.22	1232
Cu(2)-O	1260	3.29	Cu(2)	2.00	3.22	1232
O-O	1000	3.00	O(1)	−1.80	−2.70	310($\|$)
						2060($\perp$)
			O(2)	−1.80	−2.70	310($\|$)
						2060($\perp$)
			O(3)	−1.81	−2.70	310
			O(4)	−1.81	−2.70	310

phase bending of O(3), we must decrease the core-shell force constant k on the O(3) atom. Kress *et al.*[11] pointed out that the polarizability of oxygen in a Cu—O bond is very sensitive to the surrounding atomic configurations. They found that, in Y 1:2:3, the value of k of the O(1) and O(4) atoms is 1675 (in units of e^2/v, e and v are electronic charge and unit-cell volume, respectively) for the displacement along the direction normal to the Cu—O bond, while that of the O(3) and O(4) atoms must be reduced to 252 to explain the observed phonon energies. In Eu 2:2:3 a plane composed of oxygen atoms is sandwiched between two Cu-O_2 planes, being different from the case in Y 1:2:3 (see Fig. 1), which may affect the polarizability of oxygen in the Cu-O_2 plane. The decrease of the B_{1g}-mode phonon energy in Eu 2:2:3 is supposed to be caused by the enhancement of the dynamical screening in the direction normal to the Cu-O_2 plane.

By decreasing force constant k for the O(3) atom from 310 to 190, the B_{1g} phonon energy decreases to 230 cm^{-1}. Decreasing the k value further makes the vibration of Cu(2) atom unstable. The A_{1g} and B_{1g} phonon energies obtained using $k=190$ for the core-shell force constant of O(3) are also shown in Fig. 3. The two A_{1g}-mode energies where O(3) and Eu (Ce) atoms displace in the same and opposite directions become 230 and 290 cm^{-1}, respectively. In Eu 2:2:3 weak peaks with A_{1g} symmetry are observed at 217 and 290 cm^{-1} [Fig. 6(a)] and, in Er-La 2:2:3, at 210 and 277 cm^{-1} [Fig. 7(b)]. We tentatively assign these peaks to the vibration of O(3) and Eu (Er) atoms along the c axis in the same and opposite directions from the comparison with the calculated phonon energies.

It should be pointed out that the T_c of Eu 2:2:3 is around 30 K, which is considerably lower than that of Y 1:2:3 (92 K), and Er-La 2:2:3 does not even show superconductivity. The mechanism of superconductivity in cuprate superconductors is still an open question. However, it has been pointed out that the weak screening of Coulomb interaction for the displacement of ions along the c direction in the cuprate superconductors causes strong electron-phonon couplings, which has a possibility to bring about a high T_c.[5] It may be realized that the larger dynamical screening on the oxygen in the Cu-O_2 plane causes lower T_c of Eu 2:2:3 in comparison with that of Y 1:2:3 and/or destory superconductivity in Er-La 2:2:3.

Our calculation, however, cannot explain the 445-cm^{-1} peak in Eu 2:2:3 (447-cm^{-1} peak in Er-La 2:2:3). The origin of this peak is not clear. The possibility that this peak is due to the in-phase bending of O(3) atoms as well as the 440-cm^{-1} peak in Y 1:2:3 cannot be denied, though it does not agree with our preliminary calculation. Because of mixing with the vibration of lanthanide atoms, the energy of the in-phase bending of the O(3) atoms may be kept nearly equal to that of Y 1:2:3 in spite of the considerable decrease of the energy of the out-of-phase bending. Another possibility is disorder-induced origin as, e.g., the 560-cm^{-1} peak (Fig. 4). Since, in the 2:2:3-type compounds, long-range order is not formed in the Cu(1)-O plane, oxygen atoms populate randomly with an occupancy of 0.5, which may cause scattering due to phonons with Raman-forbidden symmetry or zone-edge phonons to become Raman allowed.

Disorder-induced peaks are observed at 560 cm^{-1} both in Eu 2:2:3 (Fig. 4) and in Er-La 2:2:3 (Fig. 6). In the spectra of Y 1:2:3, disorder-induced peak is observed at around 580 cm^{-1} and is ascribed to the stretching-mode vibration of oxygen in the Cu(1)-O chain.[13] The 560-cm^{-1} peak of Eu 2:2:3 (Er-La 2:2:3) may be ascribed to the stretching vibration of oxygen in the Cu(1)-O plane. The intensity of the 560-cm^{-1} peak in Eu 2:2:3 is nearly equal to that of the Raman-allowed 180-cm^{-1} peak, though the density of defects is expected to be low in our sample with good superconducting property (see Fig. 2). The random population of oxygen in the O(1) sites is supposed to cause the Cu(1)—O stretching mode to become Raman allowed.

VI. SUMMARY

Raman-scattering spectra of Eu 2:2:3 and Er-La 2:2:3 were measured at room temperature. The B_{1g}-mode phonon (out-of-phase bending of oxygen in the Cu-O_2 plane) energies were found to be around 180 cm^{-1} in both compounds, which was considerably lower than that of Y 1:2:3. A phonon-energy calculation was performed using the shell model. To explain the lower phonon energy of the B_{1g} mode, the dynamical screening on the oxygen atoms in the Cu-O_2 plane must be enlarged in the 2:2:3-type compounds in comparison with in Y 1:2:3. A_{1g}-symmetry peaks were observed at around 220, 290, 450, and 540 cm^{-1}. The 220- and 290-cm^{-1} peaks were assigned as the mixed modes of oxygen in the Cu-O_2 plane and lanthanide atom and the 540-cm^{-1} peak as the stretching vibration of apical oxygen. It was also found that Raman-forbidden peaks had comparable intensity as Raman-allowed ones probably as a result of disorder in the Cu(1)-O plane.

ACKNOWLEDGMENTS

Part of this work is supported by R&D of Basic Technology for Future Industries through the New Energy and Industrial Technology Development Organization.

[1]J. G. Bednorz and K. A. Müller, Z. Phys. B **64**, 189 (1986).
[2]K. Yvon and M. Francois, Z. Phys. B **76**, 413 (1989).
[3]J. E. Hirsch, Phys. Rev. Lett. **59**, 228 (1987); P. W. Anderson, G. Baskaran, Z. Zou, and T. Hsu, *ibid.* **58**, 2790 (1987); V. J. Emery, *ibid.* **58**, 1371 (1987).
[4]W. Weber, Phys. Rev. Lett. **58**, 1371 (1987).
[5]R. Zeyher, Z. Phys. B **80**, 187 (1990); R. E. Cohen, W. E. Pickett, and H. Krakauer, Phys. Rev. Lett. **64**, 2575 (1990).
[6]Phonon-scattering spectra of $YBa_2Cu_3O_x$ have been summarized in R. Feile, Physica C **159**, 1 (1989).

[7]R. M. MacFarlane, H. J. Rosen, and H. Seki, Solid State Commun. **63**, 831 (1987); B. Friedl, C. Thomsen, and M. Cardona, Phys. Rev. Lett. **65**, 915 (1990).
[8]H. Sawa, K. Obara, J. Akimitsu, Y. Matsui, and S. Horiuch, J. Phys. Soc. Jpn. **58**, 2252 (1989).
[9]T. Wada, A. Ichinose, Y. Yaegashi, H. Yamauchi, and S. Tanaka, Jpn. J. Appl. Phys. **28**, L1779 (1989).
[10]F. E. Bates and J. E. Eldridge, Solid State Commun. **64**, 1435 (1987); S. L. Chaplot, Phys. Rev. B **37**, 2906 (1988); S. Mase, T. Yasuda, Y. Horie, and T. Fukami, Solid State Commun. **65**, 477 (1988).
[11]W. Kress, U. Schroder, J. Prade, A. D. Kulkarni, and F. W. de Wette, Phys. Rev. B **38**, 2906 (1988).
[12]F. Beech, S. Miraglia, A. Santoro, and R. S. Roth, Phys. Rev. B **35**, 8778 (1987).
[13]R. Liu, C. Thomsen, W. Kress, M. Cardona, and B. Gegenheimer, Phys. Rev. B **37**, 7971 (1988).